# A 4+1 ARCHITECTURE FOR IN VIVO ELECTROPHYSIOLOGY VISUAL PROSTHESIS

Alejandro Barriga-Rivera[1], Calvin D. Eiber[1], Paul B. Matteucci[1], Spencer C. Chen[1],  John W. Morley[1, 2, 3], Nigel H. Lovell[1],

Gregg J. Suaning[1]

[1]Graduate School of Biomedical Engineering, University of New South Wales, Sydney, Australia

[2]School of Medical Science, University of New South Wales, Sydney, Australia

[3]School of Medicine, University of Western Sydney, Sydney, Australia

[1]a.barrigarivera@unsw.edu.au, [2]calvin.eiber@sydney.edu.au,

[3]pmatteucci@gmail.com, [4]spencer.chen@utexas.edu, [5]j.morley@uws.edu.au,

[6]n.lovell@unsw.edu.au, [7]g.suaning@unsw.edu.au

Abstract: Researchers around the globe are working towards restoring vision to the blind through the development of a visual neuroprosthesis. Overcoming physical, technical and biological limitations represents one of the main challenges for the scientific community and will eventually benefit the wellbeing of the recipients of these devices. Thus, understanding the physiological mechanisms of prosthetic vision plays a key role. In this context, in vivo electrophysiological studies are aiming to shed light on new stimulation paradigms that can potentially lead to improved visual perception. This paper describes a multi-viewpoint architecture of an experimental setup for the investigation of electrically evoked potentials in a retinal neuroprosthesis.

*Keywords:* visual prosthesis; electrophysiology; bionic eye; preclinical

## Introduction

Electrical stimulation of excitable tissue has been used to treat a broad variety of health conditions including hearing loss (Snyder, Middlebrooks, & Bonham, 2008), Parkinson's disease (Limousin et al., 1998) or fecal incontinence (Rosen, Urbarz, Holzer, Novi, & Schiessel, 2001) among others.

In particular, lessons learned from the success in cochlear implants are driving the development of visual prostheses. These devices represent a hope for the visually impaired community with nearly 40 million people profoundly blind worldwide (Pascolini & Mariotti, 2011). First attempts to electrically elicit visual perception in humans date from the 18th century (Shepherd, Shivdasani, Nayagam, Williams, & Blamey, 2013). However, the first clinical experiment was conducted by Brindley and Lewing in 1968 (Brindley & Lewin, 1968). In this study electrical stimulation of the visual cortex produced the perception of bright spots of light (phosphenes). Since then, different strategies to restore functional vision by electrical stimulation have primarily targeted cortical and retinal neurons (Habib, Cameron, Suaning, Lovell, & Morley, 2013; Suaning, Lovell, & Lehmann, 2014).

Retinal approaches aim to activate surviving retinal ganglion cells (RGCs) which are viable in pathologies such as retinitis pigmentosa or macular degeneration (Habib et al., 2013). However, the development of these devices is facing engineering, physical and biological challenges that reduce the spatial and temporal resolutions that can be delivered through electrical stimulation of the visual system (Eiber, Lovell, & Suaning, 2013). Current steering in the suprachoroidal space is being investigated as a technique to increase the performance of retinal neurostimulators by creating virtual electrodes (Dumm, Fallon, Williams, & Shivdasani, 2014) or reducing activation thresholds (Matteucci et al., 2013). These sorts of studies, both in vivo and in vitro, require complex experimental setups for which the scientific literature does not provide sufficient information. The aim of this contribution is therefore to present a laboratory setup for in vivo experimentation in retinal neurostimulation. The structure of the paper is inspired by the 4+1 architectural model described by Kruchten (Kruchten, 1995). A logical view depicts a general approach from a user's point of view addressing the main requirements of the system. A physical view presents the devices and hardware architectures required as well as the interconnection between them. The development view provides a description of the software systems, components and units from a programmer's perspective. The process view describes concurrency and

communications between software elements. And last but not least, an example of the system application is presented as the scenario.

## Logical View

Electrically evoked potentials (EEPs) following retinal neurostimulation are electrical responses elicited in the visual cortex. An electrode array is implanted close to the retina (epiretinal, subretinal or suprachoroidal) to create electric fields able to activate the RGCs (Shepherd et al., 2013). Then, a cascade of action potentials propagates through the optic nerve eventually activating the neurons of the visual cortex. A second electrode array is placed on the primary visual cortex to record the EEPs produced after stimulus delivery, as shown in figure 1. A personal computer (PC) is used to control both the retinal neurostimulator and the signal acquisition system and serves as an interface for the researcher.

*Figure 1. Description of the logical view of the experimental setup. A personal computer controls the retinal neurostimulator and stores biosignals acquired from the subject. A stimulating electrode array is implanted close to the retina whereas the recording array is located on the visual cortex.*
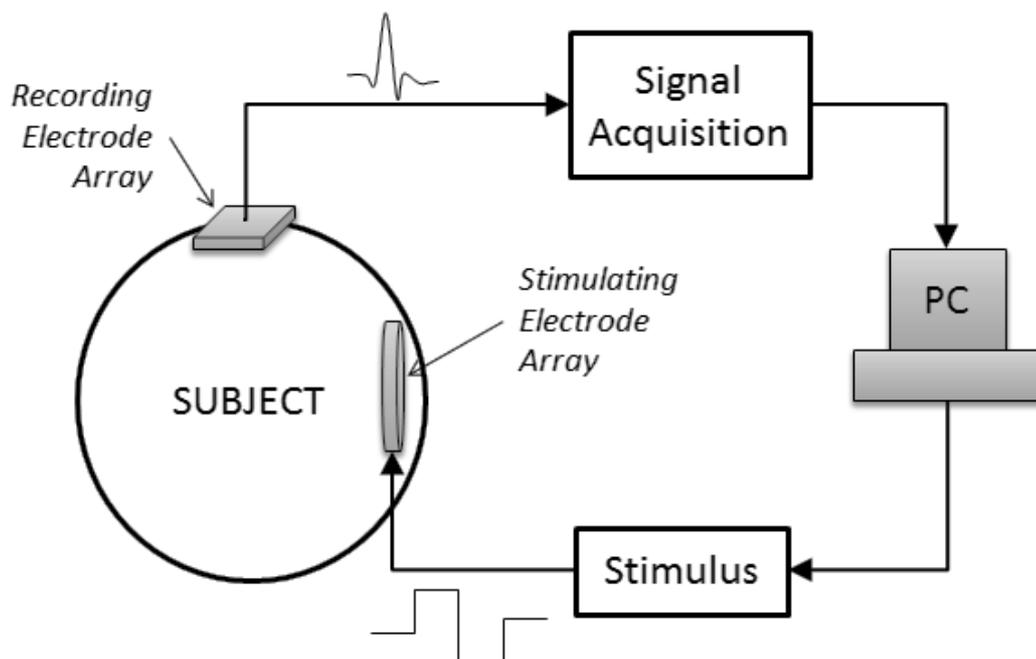


A neural stimulator consisting of a number of independent current sources connected to the stimulating electrode array allows the delivery of a repertoire of different stimulus configurations (Wong et al., 2007). The

waveform parameters are programmed on the neural stimulator through the PC. On the other hand, signals acquired from the visual cortex require the second electrode array to be interfaced to a sophisticated signal acquisition system. These signals are typically low in amplitude and therefore there is a need for using a headstage amplifier, that is, an ultralow-noise amplifier that acts as an impedance adaptor between the excitable tissue and the amplifier (Fambrini, Barreto, & Saito, 2014). Data recorded during the experiment will be stored in the PC for off-line analysis.

*Figure 2. Block diagram that illustrates the connections between the physical subsystems of the experimental setup. A personal computer controls a bioamp processor and the instrumentation platform through an optical connection (red arrows), and the stimulator by an electrically isolated USB connection. The bioamp processor is connected to the preamplifier using fibre optics and interfaces to the recording array using a headstage. The stimulator is connected to a switch matrix, and a digital multimeter records the waveforms at the stimulator site. The output of the switch matrix is connected to the stimulating array located at the retina.*
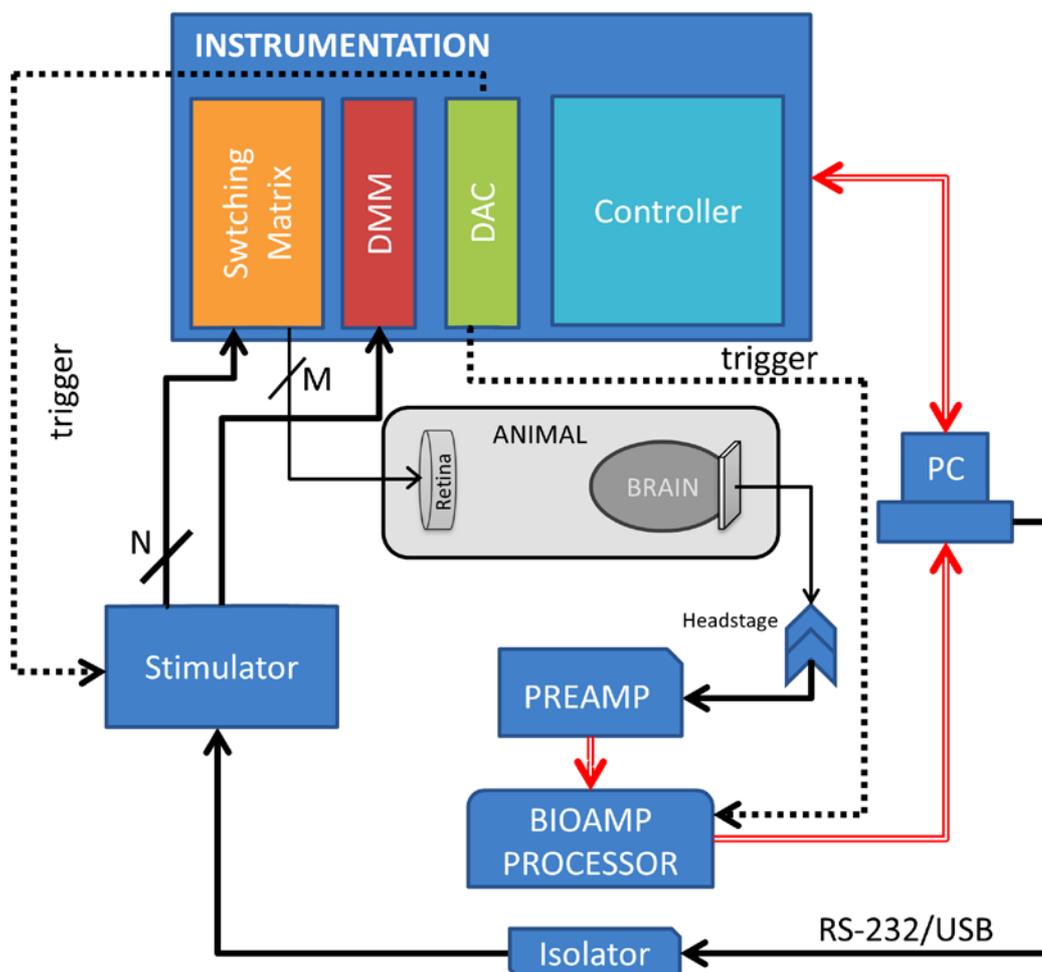
## Physical View

Both the stimulating and the recording subsystems are controlled and synchronized by the PC. This computer is optically connected to a modular instrumentation platform that generates the stimulus trigger signal, provides extra switching capabilities and digitizes the stimulus waveform to assess the impedance of the electrode-tissue interface. The PC is also optically connected to a BioAmp processor and through isolated USB to the neurostimulator. Figure 2 presents a block diagram showing the interconnections between the different hardware subsystems.

### Instrumentation platform

A National Instruments PCI eXtensions for Instrumentation (NI PXI, National Instruments Corporation, Texas, USA) provides an instrumentation platform to further the capabilities of the retinal neurostimulator.

- Chassis (NI PXI-1000B): general purpose PXI chassis with capacity for up to eight instruments.

- Controller (NI PXI-8336): this module provides control over the whole system by implementing a PCI-to-PCI bridge through an optical connection. This is a transparent link that provides electrical isolation between the PC and the PXI system. It consists of two parts, a PCI card installed on the personal computer which is to be used to control the PXI and a module connected to the main PXI chassis.

- Digital multi-meter (NI PXI-4071): high-performance digital multi-meter (DMM) able to measure voltage from ±10 nV to 1000 V, current from ±1 pA to 3 A at sampling rates up to 1.8MS/s. This device is used to record the waveforms and to estimate the impedance of the electrode-tissue interface.

- Digital-Analog Converter (NI PXI-6259): this module has four 16-bit resolution analog outputs used to generate the trigger signal for recording of the stimulus waveforms.

- Switch matrix (NI PXI-2532): this device provides 512 cross points that allows combining different current sources from the retinal neurostimulator to achieve more complex stimulus configurations.

## Retinal neurostimulator

A 98-channel neurostimulator able to activate up to 14 electrodes simultaneously was designed at the authors' laboratory (Jung et al., 2013). The system consists of 14 pairs of current sources/sinks that operate together to provide charge balance. Each pair can be switched to any of seven electrodes arranged in a hexagonal pattern to provide monopolar, bipolar, tripolar and hexapolar configurations as shown in the example of figure 3.

*Figure 3. Example illustrating different return configurations based on a hexagonal pattern. Red arrows represent the flow of electric current and hollow electrodes indicate they have been configured as the electrical return path. Hexagon A, B, C and D illustrate hexapolar, tripolar, monopolar and bipolar return configurations respectively.*
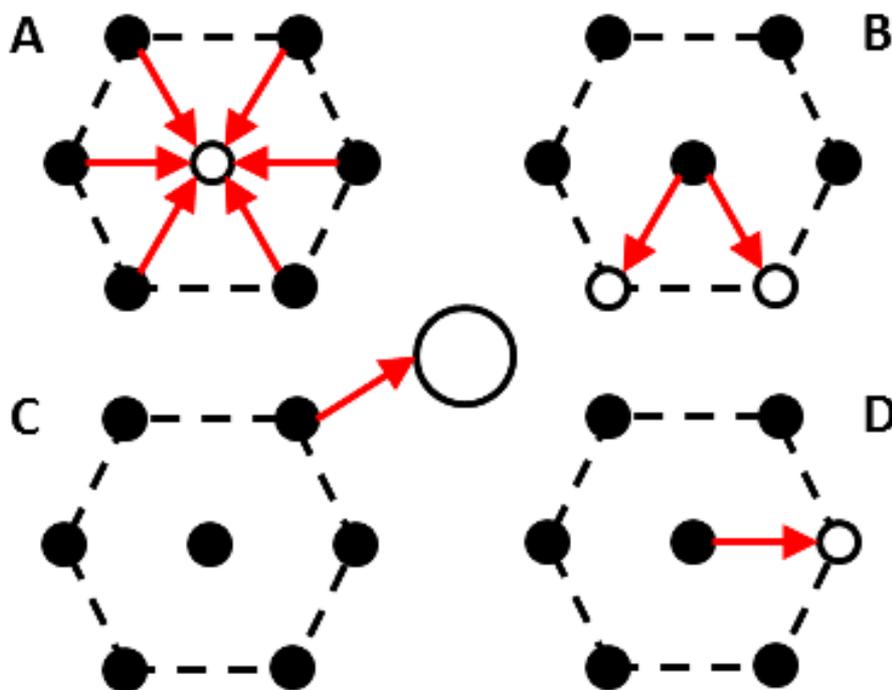


The neurostimulator is designed as an application-specific integrated circuit (ASIC) that is controlled by an ATxmega128A3U (Atmel, San Jose, California, USA) microcontroller using a serial peripheral interface (SPI) bus. The microcontroller can be programmed from the PC using RS-232 over USB.

## Signal acquisition subsystem

Three elements constitute the signal conditioning and acquisition subsystem: high-impedance headstages, a multichannel preamplifier and a bioamp processor. The following devices are manufactured by Tucker Davis Technology (Tucker Davis Technology, Florida, USA).

- Headstage (NN32AC/NN64AC): both 32-channel and 64-channel high impedance headstages are used as a recording interface. These devices provide a unity gain with an input impedance of 1014   ▫.

- Multichannel preamplifier (PZ5-128): a 128-channel digitizer records synchronized potentials from the brain. To provide electrical isolation, the preamplifier is battery powered and communicates with the processor system using a fiber optic connection. It provides a sampling rate up to 50 kHz.

- Bioamp Processor (RZ2-8): it is a signal processor comprising eight ultrafast digital signal processors that can be programmed for fast data acquisition and real-time processing.

## Stimulating electrode arrays

Retinal stimulating electrode arrays are fabricated at the authors' laboratory by laser micromachining of platinum foil positioned on a polydimethylsiloxane substrate and mechanically strengthened with a layer of polyethylene terephthalate (Dodds, Schuettler, Guenther, Lovell, & Suaning, 2011; Matteucci et al., 2013). The electrode openings are cut using the same laser micromachining technique. The exposed surface of each of the electrodes is roughened using a picosecond laser as described by Green and coworkers (Green et al., 2014). This technique extends longevity and increases the electrochemical surface area of the electrodes improving charge transfer.

## Recording electrode arrays

Cortical surface electrodes can be used to map the activity of the primary visual cortex. These electrodes are fabricated following the procedure

previously described for the stimulating electrode arrays. These electrodes can record evoked potentials. However, intracortical multi-electrode arrays are able to capture the electrical activity of single neuron and local field potentials and therefore are more pertinent to electrophysiological research. Although the system allows for both kinds of electrode arrays, results from surface electrodes are presented.

## Development View

Three main software components were developed in this experimental setup to control the retinal neurostimulator, the instrumentation platform and the signal acquisition subsystem as shown in Fig. 4.

A firmware subsystem was developed in C language to provide the ASIC chip with further capabilities. A PXI software subsystem, also written in C, initializes the instrumentation platform and provides the user with a friendly interface to program the stimulator with the stimuli to be delivered. A TDT software subsystem is implemented using Real-time Processor Visual Design Studio (RPvdsEx), a visual programming language that defines control objects to generate the circuits in the processor system. Communication between the PXI and the TDT software subsystems relies on ActiveX controls, a framework to exchange information between software applications, whereas communication between the stimulator and the PXI software uses a proprietary high level protocol over RS232.

*Figure 4. Overview of the software architecture. Three main software subsystems can be identified and related to hardware subsystems: firmware, PCI eXtensions for instrumentation (PXI) software, and Tucker Davis Technology TDT software. The firmware runs on the retinal neurostimulator, whereas the PXI and the TDT subsystems are executed on the personal computer to control the instrumentation platform and the signal acquisition system respectively.*
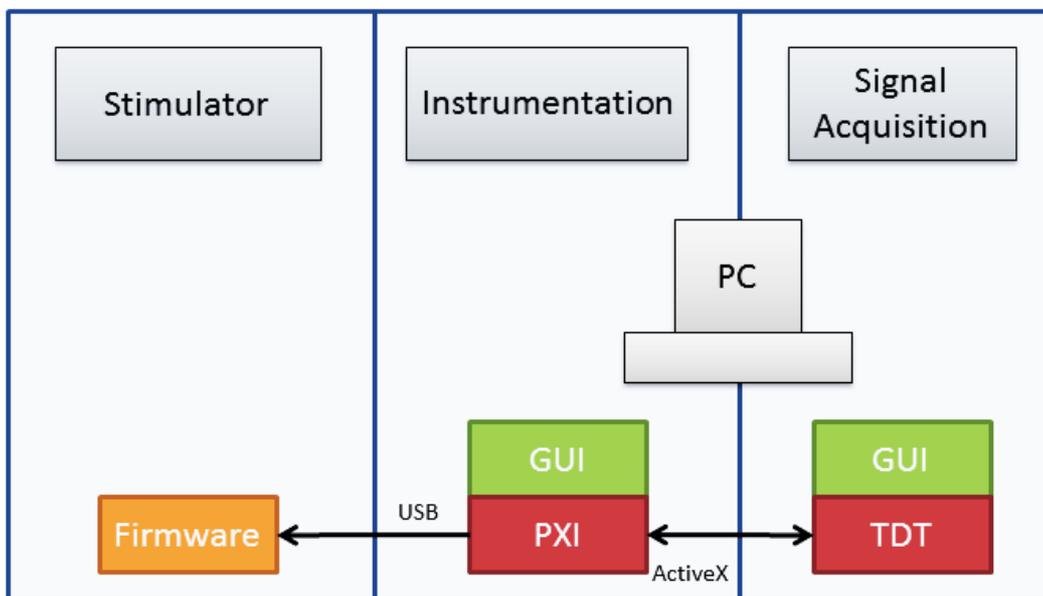


## Neurostimulator firmware

The software driving the stimulator can be described as following a layer model in which each layer is implemented in a separate C file, as in figure 5. Serial communications are carried out using a universal asynchronous receiver/transmitter (UART) unit. On top of this layer, a proprietary communication protocol enables programming the stimulus configuration in the microcontroller. Each stimulus is defined in terms of a structure of parameters that determine the current amplitude, phase and inter-phase times, symmetry of the pulse, number of stimuli per train and the return configuration. A list of stimuli is stored in memory such that the PC can indicate which stimulus is the next to be delivered after reception of the trigger signal. Finally, the upper layer translates the stimulus into a series of microinstructions which are sent through the SPI bus to the ASIC chip. This software subsystem was developed in C and compiled using Win AVR GCC compiler.

*Figure 5. Layer model of the firmware subsystem. Communication relies on USB using a UART interface. A proprietary protocol defines a series of data frames to program the stimuli to be delivered. The upper layer deals with the ASIC to deliver the chosen stimulus through a serial peripheral interface.*
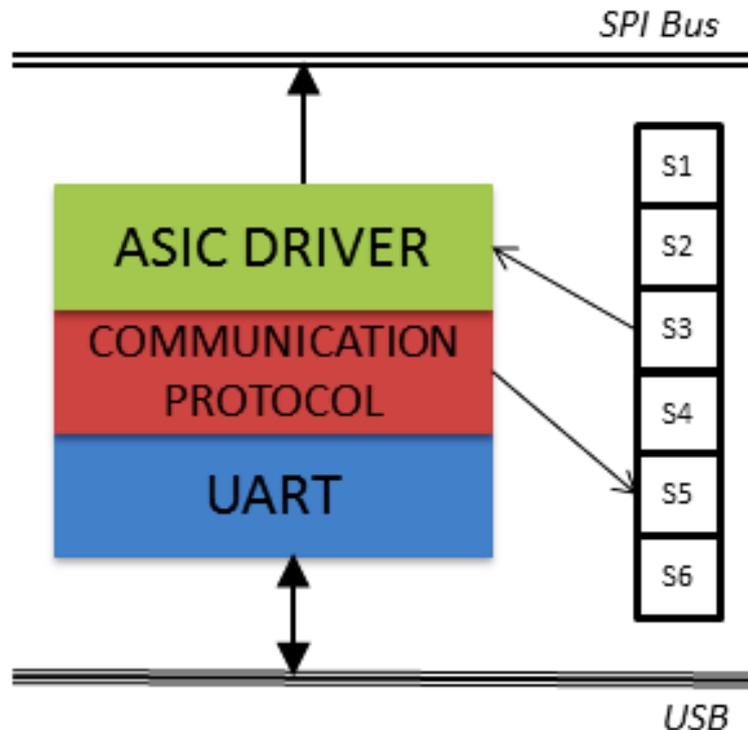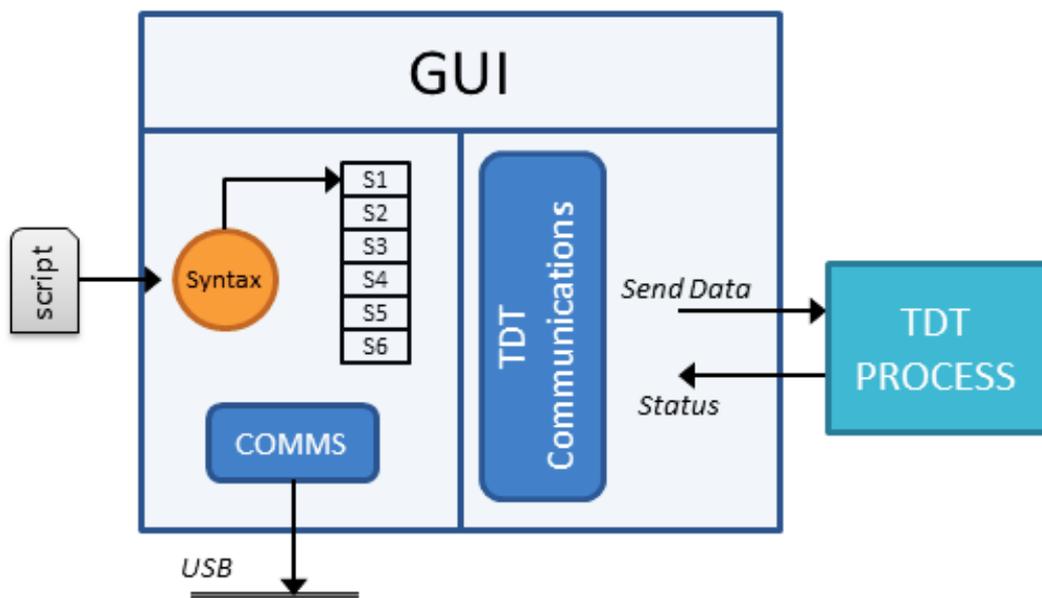


## PXI software

This software subsystem provides the primary graphical user interface (GUI). The main function initializes all the instruments and launches the GUI. The architecture of this subsystem can better be described as a modular architecture in which each module is implemented in a separate C file. On the one hand, a simulator module provides data structures for storing the set of stimuli to be programmed in the neurostimulator. These stimuli can be programmed using the GUI or through a script that is read by this module. In addition, the stimulator module implements the other end of the communication protocol between the neurostimulator and the PC. On the other hand, the TDT module of the PXI software is in charge of sending stimulus information to the TDT subsystem to be stored along with the biosignals as illustrated in figure 6.

Additionally, the GUI allows the researcher to access the switch matrix to combine the stimulating channels in a fashion such that different stimulation

strategies can be investigated. Note that this software subsystem was developed in C and compiled under Windows 7 (Microsoft, Redmond, Washington, USA) using LabWindows/CVI (National Instruments Corporation, Texas, USA).

*Figure 6. Diagram illustrating the modules that integrate the PXI software. A GUI represents the upper layer and the interface with the end user. Stimuli can be described in a file. Two different modules implement communications with the stimulator and with the TDT subsystems.*



## TDT software

The BioAmp processor provides powerful real-time signal processing capabilities. Low-level programming is normally required to optimize the performance of these kinds of devices. RPvdsEx is a tool developed by the Tucker Davis Technology that facilitates the development of applications by means of a graphical design interface. This is a visual programming language that simplifies the complexity of assembly code giving control over each digital signal processor (DSP).

*Figure 7. Task assignment per DSP. The figure illustrates which task was assigned to each processor. DSP-1 is in charge of mapping the recording array and streaming data from analog input. DSP-2 handles timing. DSP-4, DSP-5 and DSP-7 store data in the appropriate tank. Finally, DSP-6 and DSP-8 provide real-time spike detection.*
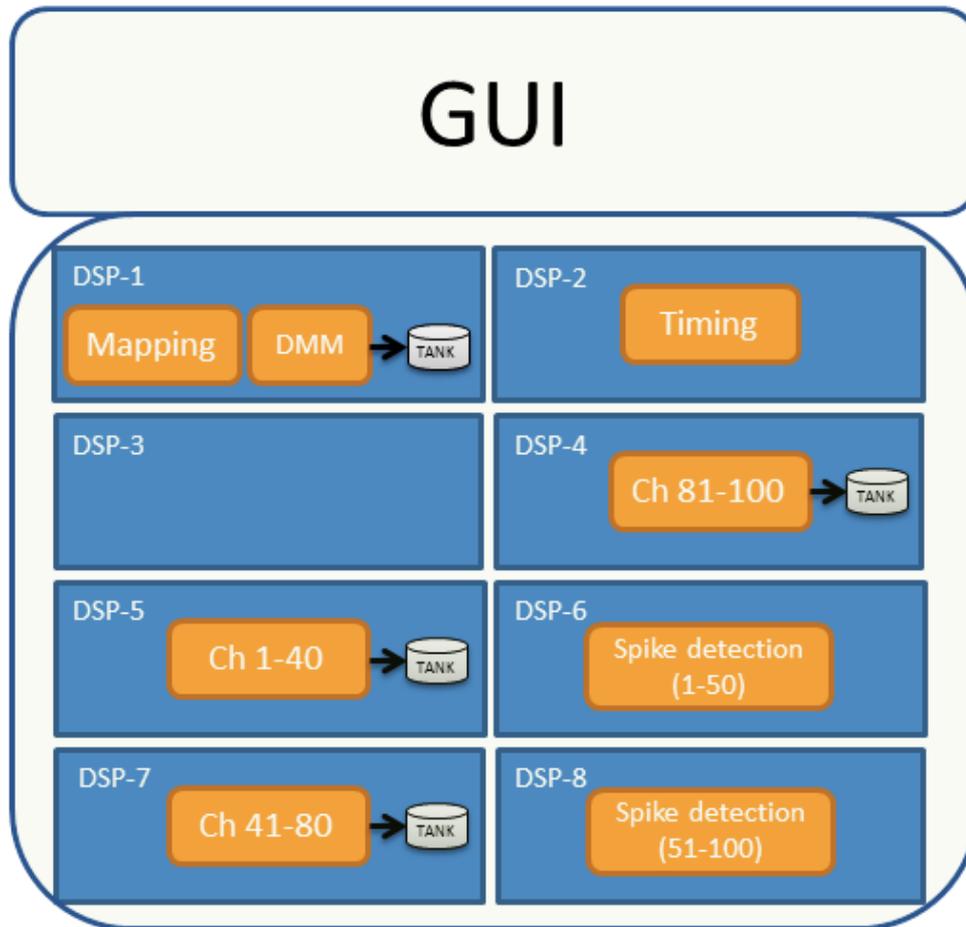


The TDT software creates a data tank which is a collection of files stored in the hard drive of the PC to where signals are streamed. Access to this information can be performed off-line. Two main conceptual layers can be identified in this subsystem. First of all, there is a GUI that allows visualization of acquired and processed signals. This interface provides control over the circuits as well. The second layer, as illustrated in figure 7, represents the tasks performed by each DSP. Five main tasks can be identified:

- Channel mapping: this is a table that switches channels in the recorded data stream to match the pinout of each recording electrode array.

- DMM: records the waveforms registered by the instrumentation platform.

- Timing: timing and control signals including the addition of timestamps to identify the onset of segments of interest within the recordings known as epochs.

- Channel streaming: stores the corresponding channel waveforms in the data tank.

- Spike detection: applies a cascade of filters to detect spikes in real time during the recording.

## Process view

First of all, the user defines the list of stimuli to be delivered by writing a file with the parameters of each stimulus or using the GUI of the PXI subsystem to build the file.

*Figure 8. Message-passing diagram illustrating the sequence of events occurring in different subsystems. After programming the simulator, the PXI subsystem indicates that stimulation is about to start. Then, it sends the stimulus identifier and the parameters of the stimulus followed by the trigger signal. This sequence is repeated until the end of the experiment.*
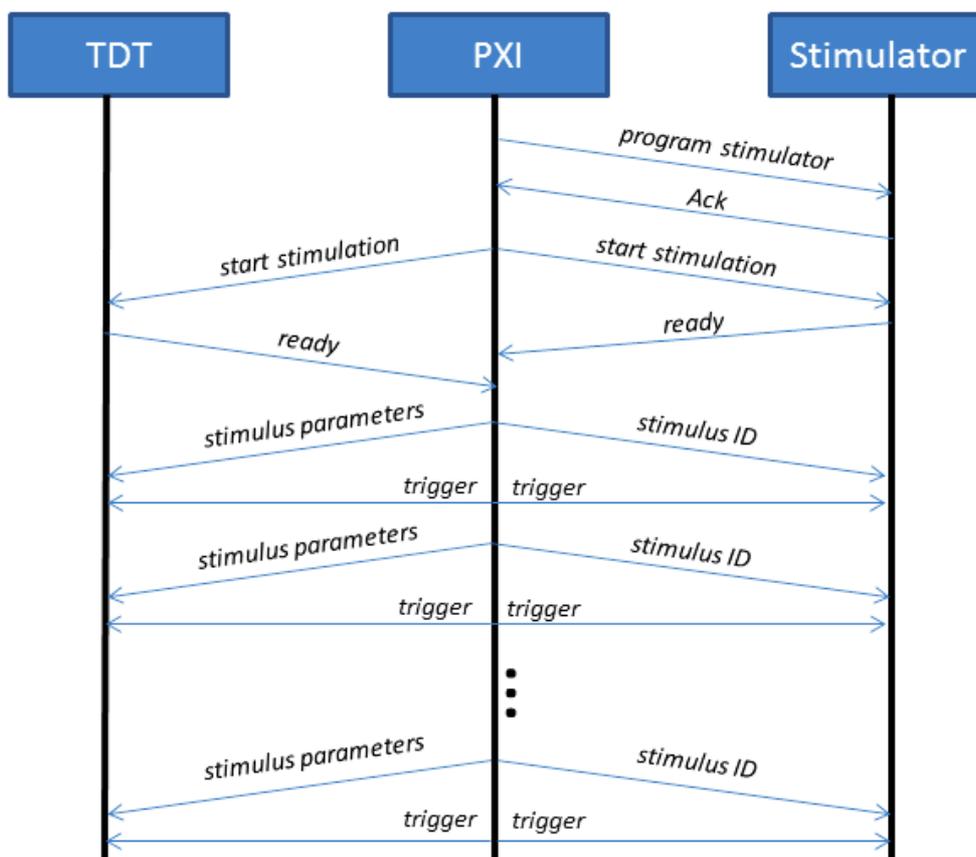
Next, the user sets the number of repetitions for each stimulus and the inter-stimulus time. In general, the arrival of stimuli is modeled as a Poisson process with an inter-stimulus time distributed uniformly around the average value within a given interval. Afterwards, the process starts and the PXI software sends the list of parameters to the stimulator as defined by the user.

Once the device is programmed, the PXI communicates to both ends that stimulation is ready to start. After receiving acknowledgement from both ends, the PXI software sends, on the one hand, the stimulus identifier to be delivered to the stimulator, and the parameters corresponding to that stimulus to the TDT subsystem, as shown in figure 8. Then, the PXI software triggers the stimulus delivery and repeats this operation accordingly until the experiment ends or the user stops the process.

## Scenario

This section presents briefly an experiment conducted at the University of New South Wales, Australia, using the setup previously described in this contribution. This section illustrates an example of the application of the system previously described. This research was approved by the UNSW Animal Care & Ethics Committee in compliance with the Australian code for care and use of animals for scientific purposes. This study adheres to the ARVO Statement for the Use of Animals in Ophthalmic and Vision Research.

### Animal preparation

In this study two normally sighted adult wethers were included. An intramuscular injection (12 mg·kg$^{-1}$) of Zoletil 100 (Virbac, Australia) was used to induce anaesthesia, which was maintained afterwards by inhalation of isofluorane (1.5-3% in 2 l·min$^{-1}$ O$_2$). Dexamethasone (1.5 mg·kg$^{-1}$) was injected intramuscularly to reduce inflammation and fluid loss was replaced by intravenous infusion of Hartman's solution. During the experiment, oxygen saturation, heart rate, blood pressure, and core temperature were continuously monitored.

A 13-electrode array arranged as two overlapping hexagons with electrode diameters between 0.4 and 1.0 mm was implanted in the suprachoroidal space of the right eye through an incision opened 10 mm posterior to the limbus. The stimulating electrode array was manufactured in the authors' laboratory following the methodology described by Schuettler and coworkers (Schuettler, Stiess, King, & Suaning, 2005) and is illustrated in figure 9A. The surfaces of the electrodes were laser-patterned to increase charge injection limits (Green et al., 2014).

*Figure 9. Panel A: stimulating electrode array consisting of 13 platinum electrodes with opening diameters of 400, 600 and 1000μm. Panel B: Infrared fundus imaging showing the optic disc (OD) and the location of the stimulating electrode array.*
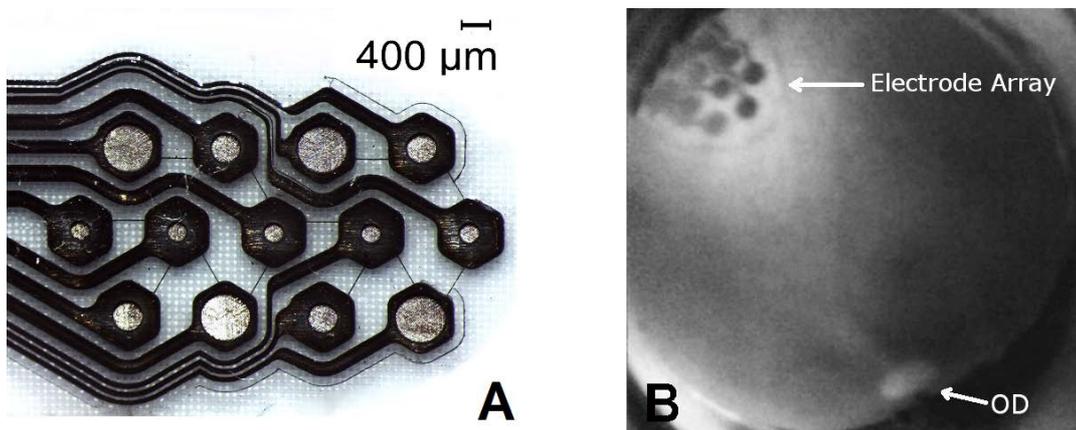


An area of the visual cortex was exposed through a craniotomy contralateral to the implanted site centered 20 mm rostral and 10 mm lateral to the lambdoid suture (Suaning, Lovell, & Kerdraon, 2001). Correct placement of the array was assessed via infra-red (940 nm) fundus imaging as illustrated in figure 9B using an in-house-built system.

Two different surface electrode arrays were used to record EEPs through the dura: a 7-electrode array from the author's lab and a 16-electrode array (IMTEK, University of Freiburg, Germany). Biphasic constant-current pulses with return set to a distant monopolar return were delivered. Charge injection was balanced and at all times remained below 210 $\mu C \cdot cm^{-2}$ in each phase. All pulses had a phase duration of 500 $\mu s$ and interphase interval of 10 $\mu s$. Inter-stimulus time was randomized between 0.75 and 1.25 s. All data were analyzed off-line using scripts written in Matlab 2013b (The MathWorks,

Massachusetts, USA) to calculate the ensemble averaging of 25 repeats. Note that the stimulus waveforms were chosen as in previous publications in cat models (Matteucci et al., 2013) and similar to those used in humans during clinical trials (Stronks, Barry, & Dagnelie, 2013).

## Results

EEPs were successfully elicited and recorded by electrically stimulating the eye of an ovine model. Figure 11 shows an example of the EEP obtained using a 7-electrode array arranged in a hexagonal pattern. One can observe the stimulation artifact occurring at t=0. Note that the most rostro-medial channel was faulty.

*Figure 10. Electrically evoked potentials recorded using a 7-electrode array arranged in a hexagonal format. Stimulation artifact can be observed at t=0. The most rostro-medial channel was faulty.*
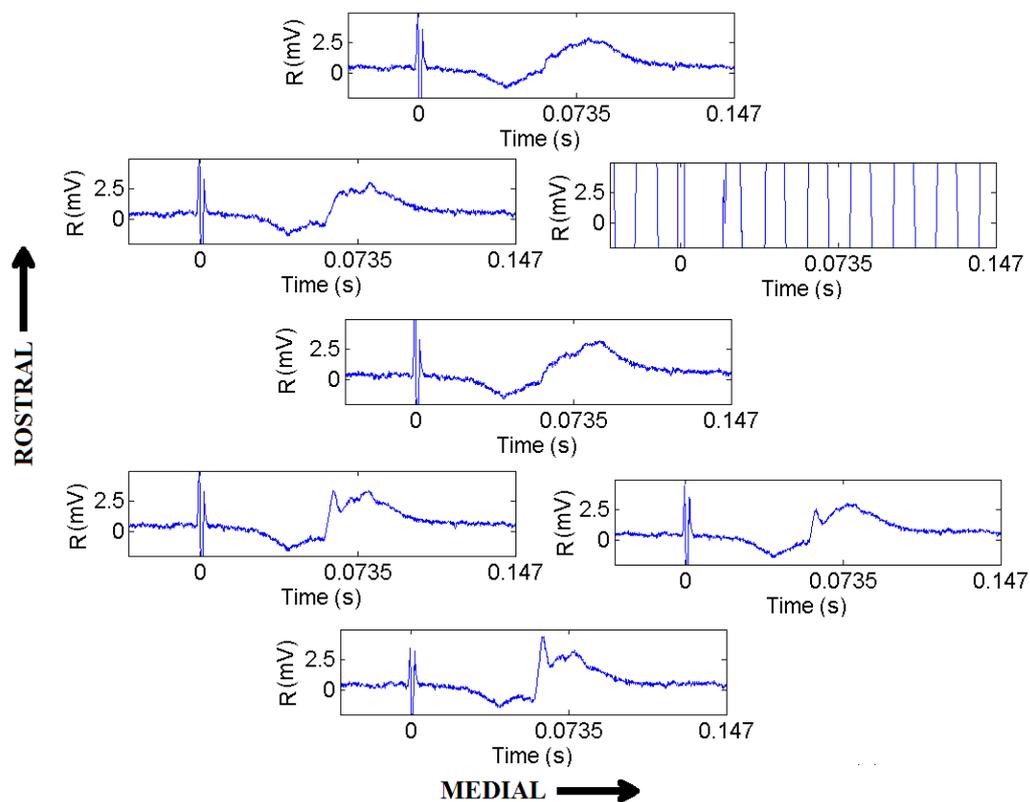


On the other hand, figure 12 shows an example of an EEP recorded with the 16-electrode array after applying a band-pass filter to remove low frequency components. In both cases, the latency between the onset of the stimulus and the peak of the response was approximately 66 ms. Stronks et al. (2013)

reported EEP in humans with latencies to first peak between 40 and 80 ms, similar to that presented in this work.

*Figure 11. Band-pass electrically evoked potentials recorded with a 16-electrode array. Stimulus artifact was recorded at t=0 in all channels with two channels with poor coupling to the cortex observable on the lateral side.*
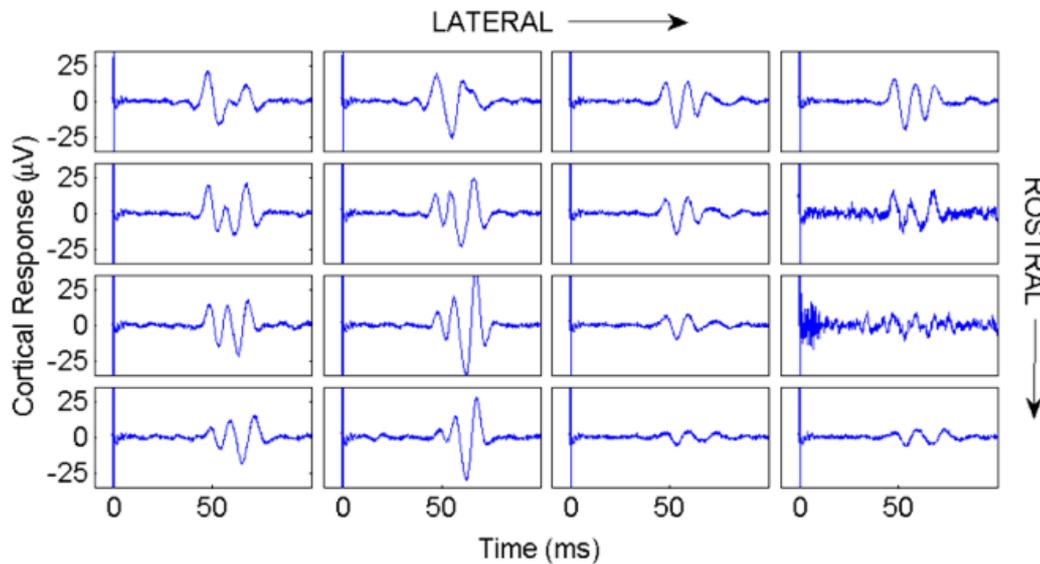


## Discussion and conclusion

The study of the electrophysiology underpinning retinal neurostimulation is a growing area of research with an important number of publications in the last few years (Eiber et al., 2013). As visual prostheses continue to develop, further understanding of current steering strategies is required to improve the performance of retinal implants (Dumm et al., 2014; Matteucci et al., 2013). This paper presents a comprehensive architectural description of an experimental setup for the investigation of visual prosthesis with the aim to facilitate other researchers to further the knowledge in this area. This four-view model does not cover low-level aspects of the design. Nevertheless, it provides sufficient information for other researchers to replicate a similar implementation. Future neural stimulators should include further switching capabilities and instruments to monitor the electrode-tissue interfaces. This would simplify the current setup and improve its usability.

Electrophysiological recordings may be impacted by a number of noise sources including electrical (such us equipment, main power line or lifts) and biological (breathing, cardiac activity or blood flow among others). Because the stimulus will create a strong artifact, it is recommended that some filtering of the neural signals be applied off-line after artifact removal. Additionally, some researchers may consider the use of Faraday cages to minimize interferences from other devices.

Results obtained from supradural recordings are comparable to those found in the scientific literature (Barriga-Rivera et al., 2015; Stronks et al., 2013; Suaning et al., 2001). This experiment shows evidence on the feasibility of retinal neurostimulation in an ovine model. The amplitude of the EEP varied in different cortical locations: higher amplitudes showed higher correlation with the retinal site where stimuli were delivered. The experimental setup described in this paper can be used to investigate the benefits derived from field shaping strategies in retinal stimulation (Dumm et al., 2014; Matteucci et al., 2013) and allows combining multiple current sources to achieve more complex current distribution patterns. It can also be used to investigate other forms of neural stimulation including high-frequency stimulation. Penetrating electrode arrays allow recording multiunit spiking activity in the visual cortex. Multi-shank probes could be used to record neural activity from lower visual centers such as the lateral geniculate nucleus or the superior colliculus. This has been used to assess the efficacy of different stimulation paradigms, particularly through the reduction of activation thresholds and the increase in visual acuity. Similar methodologies can be used to investigate other fields in neurosciences including cochlear stimulation (Fallon, Shepherd, & Irvine, 2014) or pain perception (Houzé, Bradley, Magnin, & Garcia-Larrea, 2013) among others.

## Acknowledgement

## References

[1]    Barriga-Rivera, A., Eiber C.D., Doods C.W.D., D., Fung A., Tatarinoff V., Lovel N.H. & Suaning, GJ. (2015). Electrically Evoked Potentials in an Ovine Model for the Evaluation of Visual Prosthesis Efficacy. Proceedings of the 37th Annual International Conference of the IEEE Engineering in Medicine and Biology Society (EMBC).

[2]    Brindley, G. S., & Lewin, W. (1968). The sensations produced by electrical stimulation of the visual cortex. The Journal of Physiology, 196(2), 479-493.

[3]    Dodds, C., Schuettler, M., Guenther, T., Lovell, N., & Suaning, G. (2011). Advancements in electrode design and laser techniques for fabricating micro-electrode arrays as part of a retinal prosthesis. Proceedings of the 33rd Annual International Conference of the IEEE Engineering in Medicine and Biology Society (EMBC).

[4]    Dumm, G., Fallon, J. B., Williams, C. E., & Shivdasani, M. N. (2014). Virtual Electrodes by Current Steering in Retinal Prostheses. Investigative Ophthalmology & Visual Science, 55(12), 8077-8085.

[5]    Eiber, C. D., Lovell, N. H., & Suaning, G. J. (2013). Attaining higher resolution visual prosthetics: a review of the factors and limitations. Journal of Neural Engineering, 10(1), 011002.

[6]    Fallon, J. B., Shepherd, R. K., & Irvine, D. R. (2014). Effects of chronic cochlear electrical stimulation after an extended period of profound deafness on primary auditory cortex organization in cats. European Journal of Neuroscience, 39(5), 811-820.

[7]    Fambrini, F., Barreto, M. A., & Saito, J. H. (2014). Low noise microelectrode array signal headstage pre-amplifier for in-vitro neuron culture. Proceedings of the 27th International Symposium of the IEEE Computer-Based Medical Systems (CBMS).

[8]    Green, R., Matteucci, P., Dodds, C., et al. (2014). Laser patterning of platinum electrodes for safe neurostimulation. Journal of Neural Engineering, 11(5), 056017.

[9]     Habib, A. G., Cameron, M. A., Suaning, G. J., Lovell, N. H., & Morley, J. W. (2013). Spatially restricted electrical activation of retinal ganglion cells in the rabbit retina by hexapolar electrode return configuration. Journal of Neural Engineering, 10(3), 036013.

[10]    Houzé, B., Bradley, C., Magnin, M., & Garcia-Larrea, L. (2013). Changes in sensory hand representation and pain thresholds induced by motor cortex stimulation in humans. Cerebral Cortex, 23(11), 2667-2676.

[11]    Jung, L. H., Shany, N., Emperle, A., Lehmann, T., Byrnes-Preston, P., Lovell, N. H., & Suaning, G. J. (2013). Design of Safe Two-Wire Interface-Driven Chip-Scale Neurostimulator for Visual Prosthesis. IEEE Journal of Solid-State Circuits, 48(9), 2217-2229.

[12]    Kruchten, P. B. (1995). The 4+ 1 view model of architecture. IEEE Software, 12(6), 42-50.

[13]    Limousin, P., Krack, P., Pollak, P., Benazzouz, A., Ardouin, C., Hoffmann, D., & Benabid, A.-L. (1998). Electrical stimulation of the subthalamic nucleus in advanced Parkinson's disease. New England Journal of Medicine, 339(16), 1105-1111.

[14]    Matteucci, P. B., Chen, S. C., Tsai, D., et al. (2013). Current steering in retinal stimulation via a quasimonopolar stimulation paradigm. Investigative Ophthalmology & Visual Science, 54(6), 4307-4320.

[15]    Pascolini, D., & Mariotti, S. P. (2011). Global estimates of visual impairment: 2010. British Journal of Ophthalmology, bjophthalmol-2011-300539.

[16]    Rosen, H. R., Urbarz, C., Holzer, B., Novi, G., & Schiessel, R. (2001). Sacral nerve stimulation as a treatment for fecal incontinence. Gastroenterology, 121(3), 536-541.

[17]    Schuettler, M., Stiess, S., King, B., & Suaning, G. (2005). Fabrication of implantable microelectrode arrays by laser cutting of silicone rubber and platinum foil. Journal of Neural Engineering, 2(1), S121.

[18]    Shepherd, R. K., Shivdasani, M. N., Nayagam, D. A., Williams, C. E., & Blamey, P. J. (2013). Visual prostheses for the blind. Trends in Biotechnology, 31(10), 562-571.

[19]    Snyder, R. L., Middlebrooks, J. C., & Bonham, B. H. (2008). Cochlear implant electrode configuration effects on activation threshold and tonotopic selectivity. Hearing Research, 235(1), 23-38.

[20]    Stronks, H. C., Barry, M. P., & Dagnelie, G. (2013). Electrically elicited visual evoked potentials in Argus II retinal implant wearers. Investigative Ophthalmology & Visual Science, 54(6), 3891.

[21]    Suaning, G., Lovell, N., & Lehmann, T. (2014). Neuromodulation of the retina from the suprachoroidal space: The Phoenix 99 implant. Proceedings of the 2014 IEEE Biomedical Circuits and Systems Conference (BioCAS).

[22]    Suaning, G. J., Lovell, N. H., & Kerdraon, Y. A. (2001). Physiological response in ovis aries resulting from electrical stimuli delivered by an implantable vision prosthesis. Paper presented at the Engineering in Medicine and Biology Society, 2001. Proceedings of the 23rd Annual International Conference of the IEEE Engineering in Medicine and Biology Society (EMBC).

[23]    Wong, Y. T., Dommel, N., Preston, P., Hallum, L. E., Lehmann, T., Lovell, N. H., & Suaning, G. J. (2007). Retinal neurostimulator for a multifocal vision prosthesis. IEEE Transactions on Neural Systems and Rehabilitation Engineering, 15(3), 425-434.